As published in
OutsourcedPharma.com,
May 13, 2015

Multivariate Study Design Using Short- and Long-lived Radioisotopes, *In Vivo* Positron Emission Tomography (PET/CT) and Planar Scintigraphy, and *Ex Vivo* Autoradiography to Assess Biodistribution and Pharmacokinetics of Bone-Targeting Test Material in a Canine Surgical Model

Scott Haller, MS, Director, Translational Imaging Center
MPI Research, 54943 North Main Street, Mattawan, Michigan 49071, USA

Jacob Hesterman, PhD, Senior Director, Image Analysis
inviCRO, 27 Drydock Avenue, 7th Floor West, Boston, Massachusetts 02210, USA

Abstract

Next to blood transfusions, bone is the most commonly implanted material in the human body, with an estimated 600,000 grafts performed annually. New methods for replacing bone or stimulating bone formation in disease settings, such as arthritis and acute injury, can be challenging to evaluate in traditional preclinical models. Image-guided techniques are playing an increasingly important role in evaluating the biodistribution and pharmacokinetics of drugs or drug delivery systems in this context. In combination with anatomical imaging modalities such as magnetic resonance imaging (MRI) and X-ray computed tomography (CT), molecular imaging modalities such as positron emission tomography (PET), single-photon emission computed tomography (SPECT) and planar scintigraphy allow for quantitation of radioisotopes to target and off-target tissues. Here we applied these techniques to evaluate the distribution and pharmacokinetics of a compound, dual-radiolabeled with ^{124}I and ^{125}I, in a canine pancarpal arthrodesis model.

Introduction

Delay or failure of fracture healing is a common, significant clinical problem confronting orthopaedic surgeons. Joint failure due to fatigue injuries or arthritic conditions are also common clinical presentations in orthopaedic medicine. Treatment options consist of invasive surgical techniques, such as internal and external fixation, bone grafting, and more radically, amputation. Noninvasive options include bone growth stimulation. The development of drugs or devices in this space requires the use of complex animal models to evaluate the biodistribution and pharmacokinetics of novel treatments. Various imaging platforms, such as MRI, CT, PET, planar scintigraphy, etc., can be used clinically and preclinically to assess these properties. Incorporation of noninvasive imaging modalities in drug/medical device development programs focusing on such therapeutics can provide a strategic imaging biomarker translatable between the preclinical and clinical trials. Development of an appropriate imaging biomarker strategy is often completed in preclinical trials and confirmed in Phase 0 clinical assessments. Preclinical models allow for application of both *in vivo* and *ex vivo* assessments, such as PET, planar scintigraphy, and autoradiography, which can be combined to provide quantitative or semi-quantitative biodistribution data using radiotracers, with CT providing complementary anatomical imaging. The use of *ex vivo* imaging in preclinical models provides a valuable supplement to *in vivo* imaging due to improved spatial resolution, as combined use of *in vivo* and *ex vivo* imaging drives better understanding of discrete distribution characteristics of materials. Appropriate design of preclinical imaging trials can provide datasets which are incredibly informative for clinical trial efforts and often increase the success of clinical teams.

Here we describe a model of canine pancarpal arthrodesis to evaluate the distribution and pharmacokinetics of a dual-radiolabeled compound implanted in the forelimb joint of skeletally mature hounds using *in vivo* and *ex vivo* imaging modalities. Due to the expected residence time of the specific material used in this study, both short- and long-lived radioisotopes were used to allow for acute and chronic assessment of the implanted material at the target location.

Methods

The canine model, skeletally mature hound, was selected for this study as the anatomical characteristics of the canine forelimb are comparable to that of the human, thus allowing for the use of clinical instrumentation in fixation of the pancarpal arthrodesis. Briefly, animals were anesthetized and a pancarpal arthrodesis produced by denuding the articular surfaces of the radius, radial carpal, and carpals. A pancarpal arthrodesis plate was attached to the second and third metacarpals, radial carpal, and radius, and the dual-radiolabeled (^{124}I and ^{125}I) test article was packed into both levels of the denuded joint (see Figure 1). In addition to post-surgical assessments, *in vivo* imaging was performed via focused forelimb, PET/CT scans were performed at 1, 24, 72, 168, and 336 hours post-surgery. Focused forelimb PET-only scans were performed at 8, 48, 96, 120, and 240 hours post-surgery and planar scintigraphy was performed at 21, 28, and 35 days post-surgery.

Ex vivo imaging was also completed on a cohort of animals within each treatment group. Briefly, with the pancarpal plate still in place, forelimbs were frozen and embedded in a 2% carboxymethylcellulose matrix. Control standards were then placed into the frozen blocks, blocks were serially sectioned, and high-resolution optical images were obtained for each section. Autoradioluminograms were taken at points to encompass the distal radius, carpals, and proximal metacarpals. These selected sections were mounted and exposed to phosphor imaging screens and scanned. The acquired optical images, along with the associated autoradioluminagrams, were analyzed.

Figure 1. Representative CT image demonstrates post-surgical mediolateral (**A**) and plate position in a skeletally mature hound. Coregistration PET/CT imaging data indicates position of implanted radiolabeled test material; dorsopalmar view (**B**) mediolateral view (**C**).

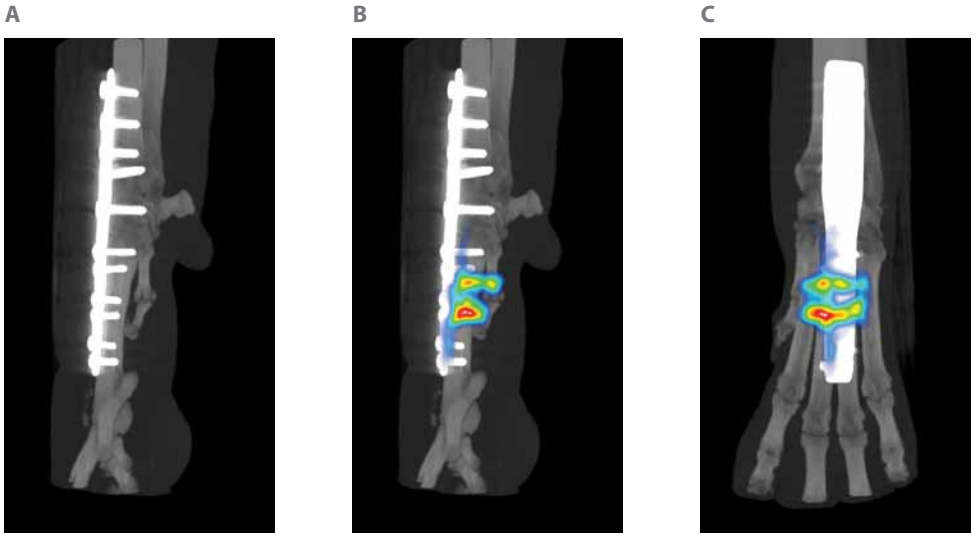

Results and Discussion

Surgical two-level pancarpal arthrodesis of the left forelimb was successfully completed in all animals assigned to study surgically. Test material, dual-labeled with ^{124}I and ^{125}I, was successfully implanted in each joint level. Animals were equally distributed across n=2 study groups—low dose and high dose ; n=10 subjects were assigned in each group.

Focused paw *in vivo* images were acquired over the course of five weeks through the use of the following modalities: PET, CT, and planar scintigraphy. PET/CT scans of ^{124}I were acquired post-operation and at 24, 72, 168, and 336 hours post-implantation. PET-only scans were acquired at 8, 48, 96, 120, and 240 hours post-implantation. Planar scintigraphy scans of ^{125}I were conducted at later time points 504, 672, and 840 hours post-implantation (days 21, 28, and 35).

Percent injected dose estimates from the *in vivo* ^{124}I PET/CT and the *in vivo* ^{125}I planar scintigraphy were successfully integrated to produce single-subject time-activity curves out to 35 days. Results at the individual subject and group level indicated clear differences between the low- and high-dose animals both qualitatively and quantitatively (Figure 2 and Figure 3). Results of the ^{125}I *ex vivo* autoradiography were consistent with *in vivo* imaging results (Figure 4). In addition to standard percent of injected dose per gram of tissue calculations for each technique, *in vivo* longitudinal data enabled calculation of pharmacokinetic parameters such as mean residence time. The residence time of the high-dose group was ~2.3X low-dose cohort residence time.

The ability to assess animals longitudinally over 35 days using noninvasive imaging detecting short- and long-lived radioisotopes reduced the total number of animals needed as compared to studies using standard histological approaches.

PET imaging and plantar scintigraphy imaging data correlated very well, and *in vivo* imaging allowed tracking of the material from beginning to end of study. *Ex vivo* autoradiography data supported *in vivo* imaging data and can be used when distribution characteristics require greater spatial resolution. Similar designs integrating surgical complexity and multiple imaging modalities may improve the predictive power of these *in vivo* models, allowing for more efficient development of implanted materials.

MPI Research
Corporate Headquarters
54943 North Main Street
Mattawan, MI 49071 USA

Tel: +1.269.668.3336
Fax: +1.269.668.4151
info@mpiresearch.com
www.mpiresearch.com

Figure 2. An aggregate time activity curve for both low- and high-dose groups (black and red, respectively) for the combined joints. This curve was generated by taking the average of all curves from each cohort. All curves were normalized to the amount of activity measured at the initial time point.

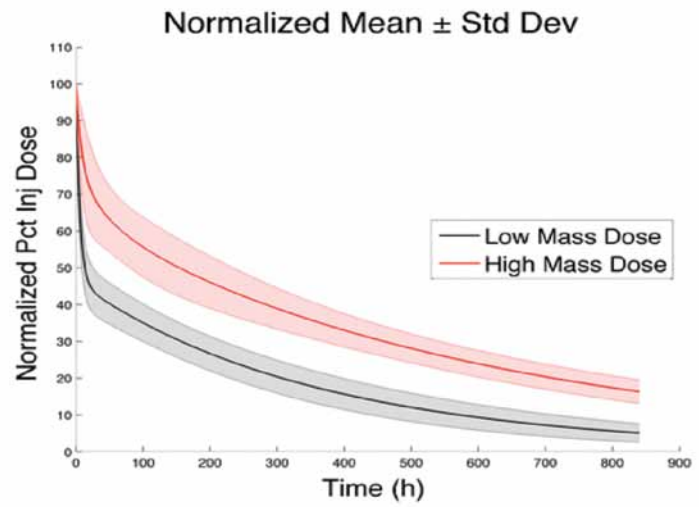

Figure 3. Representative PET/CT maximum-intensity projection images from an animal in the low-dose cohort (**A**) and high-dose cohort (**B**). Tiled image array covers scans from post-operation out to 336 hours.

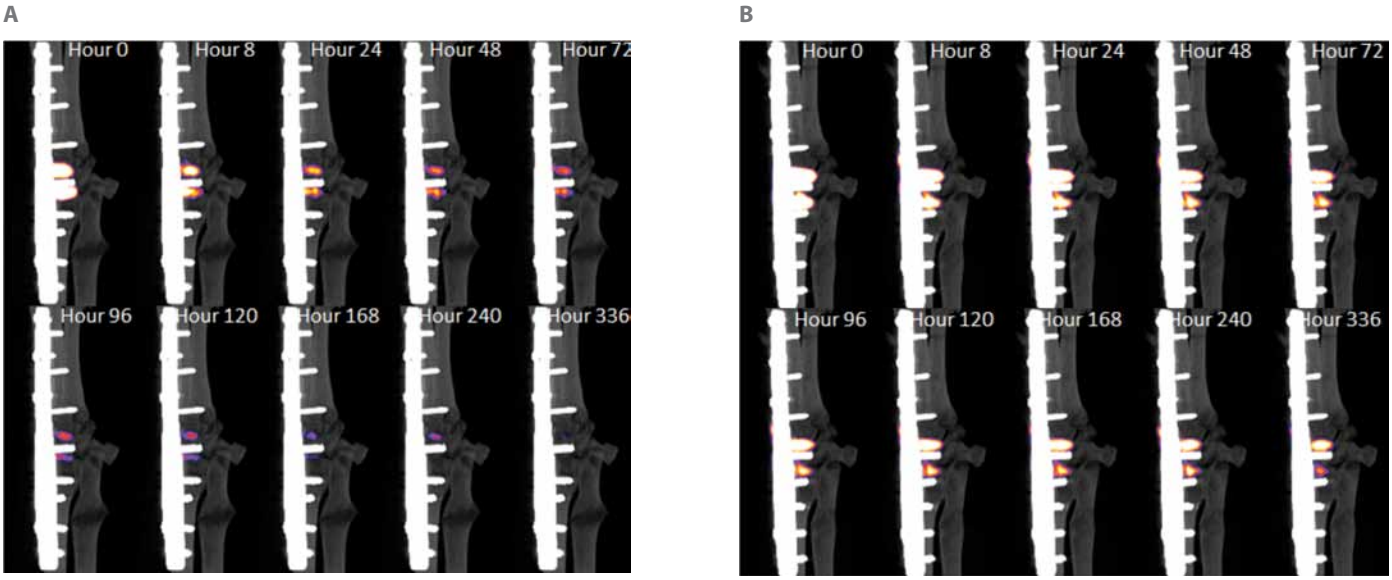

Figure 4. Representative result from quantitative autoradioluminagrams (rainbow scale) super-imposed with digital photographs (grayscale) of a paw from of low-dose cohort (**A**) and high-dose cohort (**B**). High-resolution white light images and autoradioluminogram representative of high-dose group animals (**C1**). Coregistered white light and auotradioluminogram (**C2**). Autoradioluminogram (**C3**).